



This is a pre- or post-print of an article published in
Zielonka, S., Empting, M., Könning, D., Grzeschik, J.,
Krah, S., Becker, S., Dickgießer, S., Kolmar, H.
The Shark Strikes Twice: Hypervariable Loop 2 of Shark
IgNAR Antibody Variable Domains and Its Potential to
Function as an Autonomous Paratope
(2015) Marine Biotechnology, 17 (4), pp. 386-392.

1 Short communication

2 **The shark strikes twice: Hypervariable loop 2 of shark IgNAR antibody variable domains**
3 **and its potential to function as an autonomous paratope**

4 Stefan Zielonka,¹ Martin Empting,² Doreen Könning,¹ Julius Grzeschik,³ Simon Krah,⁴ Stefan
5 Becker,⁴ Stephan Dickgießer,¹ Harald Kolmar¹⁺

6 ¹Institute for Organic Chemistry and Biochemistry, Technische Universität Darmstadt, Alarich-Weiss-Strasse 4,
7 64287 Darmstadt, Germany

8 ²Helmholtz-Institute for Pharmaceutical Research Saarland (HIPS), Department Drug Design and Optimization,
9 Saarland University, Campus C2.3, 66123 Saarbrücken, Germany

10 ³Present Address: Department of Biotechnology, University of Natural Resources and Life Science, 1190 Vienna,
11 Austria

12 ⁴Protein Engineering and Antibody Technologies, Merck-Serono, Merck KGaA, Frankfurter Straße 250, 64293
13 Darmstadt, Germany

14

15 ⁺To whom correspondence should be addressed:

16 Harald Kolmar: Institute for Organic Chemistry and Biochemistry, Technische Universität Darmstadt, Alarich-
17 Weiss-Strasse 4, D-64287 Darmstadt, Germany, Phone: +49 6151 16 4742 Fax: +49 6151 16 5399

18 Email: Kolmar@Biochemie-TUD.de

19

20 **Keywords**

21 Antibody engineering, antibody technology, shark, IgNAR, single chain binding domain, heavy
22 chain antibody, yeast surface display, antigen-binding site

23

24 **Abstract**

25 In this present study we engineered hypervariable loop 2 (HV2) of the IgNAR variable domain
26 in a way that it solely facilitates antigen binding, potentially functioning as an autonomous
27 paratope. For this, the surface exposed loop corresponding to HV2 was diversified and antigen-
28 specific vNAR molecules were isolated by library screening using yeast surface display (YSD)
29 as platform technology. An EpCAM (Epithelial cell adhesion molecule)-specific vNAR was
30 used as starting material and nine residues in HV2 were randomized. Target-specific clones
31 comprising a new HV2-mediated paratope were isolated against cluster of differentiation 3ε

32 (CD3 ϵ) and human Fc γ while retaining high affinity for EpCAM. Essentially, we demonstrate
33 that a new paratope comprising moderate affinities against a given target molecule can be
34 engineered into the vNAR scaffold that acts independent of the original antigen-binding site,
35 composed of complementarity determining region 3 (CDR3) and CDR1.

36

37 **Introduction**

38 Besides antibodies with the classical composition of heavy and light chains, sharks produce a
39 heavy-chain only homodimer, referred to as IgNAR, in which antigen binding is mediated by a
40 single variable domain, named vNAR (Greenberg et al. 1995). Due to their high affinity and
41 specificity in conjunction with their small size and high physicochemical stability, vNAR
42 domains emerged as promising molecules for biomedical and biotechnological applications and
43 consequently a plethora of antigen-specific vNAR molecules were isolated for various
44 applications, as recently reviewed (Zielonka et al. 2014a). The vNAR domain displays several
45 peculiar characteristics. By virtue of the deletion in the framework-2-CDR2-region, vNAR is
46 the smallest antibody-like antigen binding domain in the animal kingdom known to date, with
47 a molecular mass of approximately 12 kDa (Barelle et al. 2009; Stanfield et al. 2004). As a
48 consequence, vNAR domains have only two complementary determining regions CDR1 and
49 CDR3, the latter region primarily mediates antigen-binding. After antigen contact high rates of
50 mutations cluster to the CDRs, to the CDR2 truncation site, where the remaining loop forms a
51 belt-like structure at the bottom of the molecule and to a loop which corresponds to HV4 in T-
52 cell receptors (Fig. 1). Correspondingly, these mutation-prone regions have been named HV2
53 and HV4, respectively (Dooley et al. 2006; Zielonka et al. 2014a). vNAR domains can be
54 categorized into four types, based on the presence and absence of non-canonical cysteine
55 residues, which are not found in classical antibody variable domains (Diaz et al. 2002;
56 Kovalenko et al. 2013; Stanfield et al. 2004; Stanfield et al. 2007; Streltsov et al. 2005; Zielonka
57 et al. 2014a). Except for type I domains, HV2 is located distantly from the conventional antigen-
58 binding site, composed of CDR3, CDR1 and HV4 (Fig. 1). However, for type I vNAR
59 molecules, CDR3 is held tightly into the direction of HV2 (Stanfield et al. 2004). Consistent
60 with this structural feature, mutations are favored in this loop for this particular type of domain,
61 indicating that in this context HV2 might participate in antigen binding (Flajnik et al. 2011;
62 Stanfield et al. 2004).

63 Within this work, we set out to engineer HV2 in a type IV vNAR in a way that it solely
64 facilitates antigen binding, independent from the conventional antigen-binding site composed
65 of CDR3 and CDR1 (and HV4). For this, we randomized nine residues of HV2 of a high-affinity

66 EpCAM-binding semi-synthetic vNAR molecule, known as 5005 (Zielonka et al. 2014b). This
67 particular molecule was isolated from a semisynthetic library where the regions corresponding
68 to CDR1 and CDR3 were randomized. Hence, HV2 is not involved in antigen binding. Herein
69 we report the isolation of antigen-binding vNAR molecules with artificial HV2 loops against
70 two different antigens, CD3 ϵ and non-glycosylated human Fc γ , using yeast surface display.
71 Interestingly, isolated binders retained high affinities against EpCAM, demonstrating that HV2
72 can potentially function as a paratope without compromising the structural and functional
73 integrity of the vNAR scaffold. To the best of our knowledge, this approach for the generation
74 of a new antigen-binding site has not been reported to date.

75

76 **Materials and Methods**

77 *Media and reagents*

78 YPD medium contained 20 g/L tryptone, 20 g/L dextrose and 10 g/L yeast extract. SD-CAA
79 medium was composed of 1.7 g/L yeast nitrogen base without amino acids and ammonium
80 sulfate, 5 g/L ammonium sulfate, 5 g/L Bacto casamino acids, 20 g/L dextrose, 8.6 g/L
81 NaH₂PO₄ x H₂O, and 5.4 g/L Na₂HPO₄. SG-CAA medium was prepared similarly except for
82 the substitution of 20 g/L dextrose by galactose. Additionally 10 % (w/v) polyethylene glycol
83 8000 (PEG 8000) was incorporated. Phosphate-buffered saline (PBS) contained 8.1 g/L NaCl,
84 0.75 g/L KCl, 1.13 g/L Na₂HPO₄ and 0.27 g/L KH₂PO₄, pH 7.4.

85 Recombinant human His-tagged EpCAM and recombinant human CD3 ϵ were purchased from
86 AcroBiosystems. Glycosylated human Fc γ was produced in-house. Non glycosylated human
87 Fc γ , produced in-house, carries an Asn297Ala mutation, preventing glycosylation.

88

89 *Library construction*

90 pCT plasmid, carrying genetic information for EpCAM-specific vNAR molecule 5005
91 (Zielonka et al., 2014a) was used as template for HV2-randomized library construction. HV2-
92 diversification was executed in a consecutive 2-step splicing by overlap extension polymerase
93 chain reaction (PCR) as depicted in Fig. 2A. For all reactions the conditions were: 94 °C for
94 2 min, 35 cycles of 30 s at 94 °C, 30 s at 55 °C and 40 s at 72 °C, followed by 72 °C for 7 min.
95 Primer sequences are listed in Tab. S1. For the first PCR step, two reactions were carried out
96 in parallel, each containing isolated plasmid DNA as starting material. In one reaction, primer
97 pair HV2_SOE_rand_up/pCT_Seq_lo was used. The forward primer randomized 9 residues in
98 the surface exposed loop, corresponding to HV2. Residues considered for randomization are
99 shown in Fig. 1. In the other reaction, primer pair pCT_Seq_up/HV2_SOE_lo was engaged.

100 The respective PCR products were purified using Wizard® SV Gel and PCR Clean-up System
101 (Promega) according to the manufacturer's instructions. For the subsequent PCR, 1 µl of each
102 PCR product was used as template, respectively. After 6 cycles, primer pair
103 pCT_Seq_up/pCT_Seq_lo was added. The resulting PCR product was purified *via* Wizard®
104 SV Gel and PCR Clean-up System.

105 The pCT plasmid (Boder and Wittrup 1997), used for gap repair cloning and surface
106 presentation of vNAR library candidates, was digested with *NheI* and *BamHI* and purified *via*
107 Wizard® SV Gel and PCR Clean-up System. For electroporation, 1-2 µg of the digested
108 plasmid and 6-8 µg of insert were used. After 1 h incubation at 30 °C (1:1 YPD and 1 M
109 sorbitol) library size was calculated by dilution plating. Yeast cells (EBY 100) were transferred
110 into SD-CAA medium. Stocks were stored at -80 °C. For yeast surface display cells were grown
111 overnight at 30 °C in SD-CAA medium, transferred into SG-CAA medium and incubated for
112 1-2 days at 20 °C.

113

114 *Binding assays on the yeast surface and library screening for the isolation of target-specific*
115 *vNAR molecules*

116 Procedures and protocols for yeast surface display of vNAR domains have already been
117 described by our group (Zielonka et al. 2014b) and thus are herein only briefly described. Flow
118 cytometry was used to analyze presentation on the yeast surface and for single clone analysis.
119 About 10⁷ cells were labeled consecutively with anti-cMyc antibody (monoclonal, mouse, made
120 in-house) and anti-mouse IgG FITC conjugate (goat, Sigma Aldrich, diluted 1:10 in PBS) for
121 at least 10 min on ice. For single clone analysis, vNAR-presenting cells were either incubated
122 with biotinylated, His-tagged CD3ε or Fcγ antigen for 15 min on ice and subsequently stained
123 with Steptavidin-APC (diluted 1:10), Penta-His Alexa Fluor 488 conjugate (Qiagen, diluted
124 1:30) or anti-Hu IgG (Fcγ-specific) PE (eBioscience, diluted 1:30) for 10 min. Plasmid DNA
125 from positive clones was isolated and sent out for sequencing with pCT-seq_lo or pCT-seq_up
126 oligonucleotide (Tab. S1).

127 Affinities of isolated vNAR variants on yeast cells were determined as described (Chao et al.
128 2006; VanAntwerp and Wittrup 2000; Zielonka et al. 2014b). Flow cytometric analysis was
129 performed to determine antigen binding. At least eight different antigen concentrations were
130 used and cells were incubated for at least 1 h with the respective antigen. For the final
131 calculation, RFU was plotted against antigen concentration.

132 Library screening for the isolation of antigen-specific vNAR molecules was performed on a
133 MoFlo cell sorter (Beckman Coulter) and analyzed *via* Summit 4.3. For two-dimensional

134 screening, cells were resuspended in PBS containing the desired concentrations of both antigens
135 and incubated on ice for at least 30 min. Subsequently, antigen-binding was detected using
136 streptavidin-allophycocyanin conjugate (diluted 1:10), Penta-His Alexa Fluor 488 conjugate,
137 anti-Hu IgG (Fc γ -specific) PE or Fc γ -specific Fab-fragment conjugated to Alexa Fluor 488
138 (Jackson ImmunoResearch, diluted 1:30). For the first rounds of sorting of the initial library,
139 approximately 2×10^8 cells were analyzed and sorted. Consecutive rounds were at least
140 performed with a 10-fold excess of cells that were collected in the previous round to ensure
141 coverage of the enriched population.

142

143 **Results and Discussion**

144 The artificial HV2-randomized library for yeast surface display was constructed by polymerase
145 chain reaction (PCR) using plasmid encoded EpCAM-specific clone 5005 as starting material.
146 In the framework of this clone, 9 residues in HV2 were totally diversified by the incorporation
147 of trinucleotide mixtures encoding all 19 amino acids except cysteine into the corresponding
148 oligonucleotide. Residues considered for library design are given in Fig. 1 (blue residues). The
149 library was established in a consecutive 2-step splicing by overlap extension PCR, as depicted
150 in Fig. 2A and a yeast surface display library with an estimated diversity of approximately
151 1×10^9 unique clones (calculated by dilution plating) was constructed in a homologous
152 recombination-based process referred to as plasmid gap repair (Benatuil et al. 2010). As already
153 described (Zielonka et al. 2014b), library encoded HV2-randomized vNAR fragments were
154 displayed on the yeast surface *via* Aga1p/Aga2p association (Boder and Wittrup 1997). vNARs
155 were expressed as fusion protein with HA-tag and cMyc-epitope at the N-terminus and C-
156 terminus, respectively, for the detection of surface displayed library candidates. Surface
157 presentation as well as maintenance of structural integrity i.e. EpCAM-binding of HV2-
158 randomized library candidates was assessed by indirect fluorescence labeling of the cMyc-
159 epitope or *via* EpCAM binding assays on the yeast surface (Fig. 2B and C). Within one day
160 post induction, there was more than 40 % cMyc-tag expression of the library detectable and
161 about 36 % of EpCAM labeling, indicating that the vast majority of displayed vNAR fragments
162 retained their structural integrity after randomization of HV2. These findings are consistent with
163 the observation that HV2 is a mutation-prone region (Dooley et al. 2006; Flajnik et al. 2011;
164 Stanfield et al. 2004), potentially tolerating a high degree of diversity at the sequence level as
165 well as structural multiplicity.

166 To evaluate whether this loop can potentially function as a distinct antigen-binding site, the
167 library was screened against two different targets, CD3 ϵ and non-glycosylated human Fc γ . To

168 isolate binders, targeting a new antigen with HV2 while retaining affinity against EpCAM, first
169 and last round of screening were performed two-dimensionally for target-binding (Fig. 3). To
170 this end, vNAR binding of his-tagged EpCAM was detected using an Alexa Fluor 488 labeled
171 anti-His-tag antibody. Binding to CD3 ϵ was detected using biotinylated antigen as well as
172 Streptavidin-APC. To avoid off-target binding against detection reagents, the labeling strategy
173 was alternated from using biotinylated CD3 ϵ to his-tagged antigen which was detected via
174 Alexa Fluor 488 labeled anti-His-tag antibody. Consequently, we only sorted for CD3 ϵ -binding.
175 Initial FACS sorting rounds were performed with 1 μ M EpCAM and 2 μ M CD3 ϵ . To enhance
176 screening stringency, hence, to obtain binders against CD3 ϵ displaying adequate affinities, the
177 respective target protein concentration was reduced to 1 μ M in rounds 3 and 4. As shown in
178 Fig. 3, we were able to enrich cells displaying a double-positive antigen-specific signal for
179 EpCAM and CD3 ϵ within four rounds of FACS sorting. Interestingly, we also enriched for a
180 population which lost its ability for EpCAM binding, indicating that this particular population
181 lost its structural integrity (Fig. 3).

182 Likewise, sorting carried out against non-glycosylated human Fc γ protein also revealed a
183 significant enrichment of FACS double-positive clones (Fig. S1). In these particular screening
184 experiments, binding to human Fc γ was detected using either anti-human Fc γ -specific IgG
185 conjugated to PE (rounds 1,3 and 4) or Fc γ -specific Fab-fragment conjugated to Alexa Fluor
186 488 (sorting round 2).

187 Single clones were analyzed in terms of their ability to target both antigens, EpCAM and CD3 ϵ ,
188 and double-positive clones were sent out for sequencing, resulting in the identification of
189 several double-positive clones (Fig. S2). Importantly, all identified clones were direct progenies
190 of parental molecule 5005, each comprising a unique sequence in HV2, resulting from library
191 design. Most of the clones still bound strongly to EpCAM at a concentration of 1 μ M but
192 binding to CD3 ϵ was very weak at 1 μ M, as exemplarily shown for single clone H5 (Fig. S3).
193 Notwithstanding, for one clone, referred to as clone B1 we observed binding to CD3 ϵ to a
194 significantly higher extent compared to all other analyzed clones, whereas for parental molecule
195 5005 no binding was observed against CD3 ϵ at the highest concentration tested (Fig. 4). Since
196 it was evidenced that yeast surface display allows for the instantaneous characterization of
197 isolated binders in terms of affinity and stability without the need for soluble expression
198 (Doerner et al. 2014; Gai and Wittrup 2007; VanAntwerp and Wittrup 2000; Zielonka et al.
199 2014b) we decided to determine equilibrium binding constants *via* affinity titration on cells, as
200 given in Tab. 1. Binder B1 displayed affinities for CD3 ϵ of about 400 nM, without significantly
201 compromising the affinity against EpCAM, compared to its parental molecule 5005.

202 Importantly, selectivity assays conducted on the yeast surface revealed that no nonspecific
203 binding was observable against unrelated target proteins (**Fig. S4**).

204 Akin to these observations, one double positive EpCAM- and human Fc γ -binding clone,
205 referred to as clone F1 was identified after single clone analysis (Fig. S2). Characterization of
206 this clone resulted in a moderate affinity against human Fc γ of approximately 2.6 μ M.
207 Furthermore, no significant off-target binding was detected against unrelated target proteins
208 (**Fig. S4**). Affinity against EpCAM was comparable to that of its parental clone 5005, which
209 does not display detectable binding to human Fc γ , as listed in Tab. 1. In this respect, no efforts
210 were made to optimize affinities against Fc γ *via* alanine-scanning and sub-library screening.
211 Interestingly, this clone only bound to non-glycosylated human Fc γ . For the glycosylated
212 equivalent we were unable to detect any binding at the highest concentrations tested (Fig. 5).
213 Hence, one can draw conclusions with regard to the epitope that is addressed by clone F1. It is
214 tempting to speculate, that position 297 of Fc γ is involved in the vNAR-target-interaction, since
215 for wild-type Fc γ , this residue is Asn which is typically glycosylated. However, unglycosylated
216 Fc γ contains an Asn to Ala mutation at this position and it can be assumed that this mutation,
217 that prevents glycosylation, is part of the epitope targeted by HV2-diversified clone F1. Another
218 hypothesis is that glycosylation of the Fc-fragment covers the epitope targeted by
219 α -EpCAM-Fc γ -vNAR F1 in a way that this region is structurally not accessible.

220 The immunoglobulin family displays a paramount tolerability in loop length as well as sequence
221 variation, which is most evident for CDR regions of variable domains. However, this feature is
222 a general hallmark of the immunoglobulin domains (Halaby et al. 1999; Wozniak-Knopp et al.
223 2010) and loop regions other than the natural CDRs can be considered for engineering novel
224 binding characteristics. In this respect, surface-exposed loops at the N-terminal tip of CH2 of
225 human IgG have been engineered for antigen binding (Xiao et al. 2009). In another very elegant
226 approach, established by R uker and co-workers, a new antigen-binding site was introduced in
227 loop regions of the CH3 domain of human IgG (Wozniak-Knopp et al. 2010). Most importantly,
228 those engineered Fc fragments, named Fcab, retained the ability to elicit effector functions,
229 clearly indicating the structural integrity of the molecule.

230 Essentially, our study demonstrates that the vNAR scaffold can be engineered in a way that
231 HV2 potentially functions as an independent paratope, exclusively facilitating antigen binding
232 against a target-protein. Importantly the establishment of a new antigen binding site does not
233 impair the conventional antigen-binding site, composed of CDR3 and CDR1 in its affinity.
234 However, it needs to be mentioned that affinities mediated by HV2 are only moderate and
235 almost certainly require optimization for further studies such as effector cell recruitment assays.

236 In this respect, affinity maturation might be performed by second generation randomization of
237 the HV2-adjacent surface exposed loop, referred to as EF-loop, as already described by
238 Wozniak-Knopp *et al.* for human constant CH3 domains (Wozniak-Knopp et al. 2010). This
239 group utilized the EF-loop in CH3 as part of a novel antigen-binding site.

240 In recent years, bispecific antibodies and antibody domains have
241 opened new avenues for the treatment of various diseases (Kontermann 2012; Weidle et al.
242 2014). Ultimately, it remains to be elucidated, whether shark-derived antibody domains may
243 contribute to this continuously evolving field of therapeutic drug design in the future.

244

245 **Disclosure of Potential Conflicts of Interest**

246 The authors declare no potential conflicts of interest.

247

248 **Acknowledgments**

249 This work was supported in part by Federal Ministry of Education and Research (BMBF) in
250 frame of the consortium Nanokat. We thank Prof. Dr. Siegfried Neumann for general advice.

251

252 **References**

- 253 Barelle C, Gill DS, Charlton K (2009) Shark novel antigen receptors--the next generation of
254 biologic therapeutics? *Adv Exp Med Biol* 655:49-62 doi:10.1007/978-1-4419-1132-2_6
- 255 Benatuil L, Perez JM, Belk J, Hsieh CM (2010) An improved yeast transformation method for
256 the generation of very large human antibody libraries *Protein engineering, design & selection:*
257 *PEDS* 23:155-159 doi:10.1093/protein/gzq002
- 258 Boder ET, Wittrup KD (1997) Yeast surface display for screening combinatorial polypeptide
259 libraries *Nature biotechnology* 15:553-557 doi:10.1038/nbt0697-553
- 260 Chao G, Lau WL, Hackel BJ, Sazinsky SL, Lippow SM, Wittrup KD (2006) Isolating and
261 engineering human antibodies using yeast surface display *Nature protocols* 1:755-768
262 doi:10.1038/nprot.2006.94
- 263 Diaz M, Stanfield RL, Greenberg AS, Flajnik MF (2002) Structural analysis, selection, and
264 ontogeny of the shark new antigen receptor (IgNAR): identification of a new locus
265 preferentially expressed in early development *Immunogenetics* 54:501-512
266 doi:10.1007/s00251-002-0479-z
- 267 Doerner A, Rhiel L, Zielonka S, Kolmar H (2014) Therapeutic antibody engineering by high
268 efficiency cell screening *FEBS letters* 588:278-287 doi:10.1016/j.febslet.2013.11.025

269 Dooley H, Stanfield RL, Brady RA, Flajnik MF (2006) First molecular and biochemical
270 analysis of in vivo affinity maturation in an ectothermic vertebrate Proceedings of the
271 National Academy of Sciences of the United States of America 103:1846-1851
272 doi:10.1073/pnas.0508341103

273 Flajnik MF, Deschacht N, Muyldermans S (2011) A case of convergence: why did a simple
274 alternative to canonical antibodies arise in sharks and camels? PLoS biology 9:e1001120
275 doi:10.1371/journal.pbio.1001120

276 Gai SA, Wittrup KD (2007) Yeast surface display for protein engineering and characterization
277 Current opinion in structural biology 17:467-473 doi:10.1016/j.sbi.2007.08.012

278 Greenberg AS, Avila D, Hughes M, Hughes A, McKinney EC, Flajnik MF (1995) A new
279 antigen receptor gene family that undergoes rearrangement and extensive somatic
280 diversification in sharks Nature 374:168-173 doi:10.1038/374168a0

281 Halaby DM, Poupon A, Mornon J (1999) The immunoglobulin fold family: sequence analysis
282 and 3D structure comparisons Protein engineering 12:563-571

283 Kontermann RE (2012) Dual targeting strategies with bispecific antibodies mAbs 4:182-197
284 doi:10.4161/mabs.4.2.19000

285 Kovalenko OV et al. (2013) Atypical antigen recognition mode of a shark immunoglobulin
286 new antigen receptor (IgNAR) variable domain characterized by humanization and structural
287 analysis The Journal of biological chemistry 288:17408-17419 doi:10.1074/jbc.M112.435289

288 Krieger E et al. (2009) Improving physical realism, stereochemistry, and side-chain accuracy
289 in homology modeling: Four approaches that performed well in CASP8 Proteins 77 Suppl
290 9:114-122 doi:10.1002/prot.22570

291 Stanfield RL, Dooley H, Flajnik MF, Wilson IA (2004) Crystal structure of a shark single-
292 domain antibody V region in complex with lysozyme Science 305:1770-1773
293 doi:10.1126/science.1101148

294 Stanfield RL, Dooley H, Verdino P, Flajnik MF, Wilson IA (2007) Maturation of shark
295 single-domain (IgNAR) antibodies: evidence for induced-fit binding Journal of molecular
296 biology 367:358-372 doi:10.1016/j.jmb.2006.12.045

297 Streltsov VA, Carmichael JA, Nuttall SD (2005) Structure of a shark IgNAR antibody
298 variable domain and modeling of an early-developmental isotype Protein science : a
299 publication of the Protein Society 14:2901-2909 doi:10.1110/ps.051709505

300 VanAntwerp JJ, Wittrup KD (2000) Fine affinity discrimination by yeast surface display and
301 flow cytometry Biotechnology progress 16:31-37 doi:10.1021/bp990133s

302 Weidle UH, Kontermann RE, Brinkmann U (2014) Tumor-antigen-binding bispecific
303 antibodies for cancer treatment *Semin Oncol* 41:653-660
304 doi:10.1053/j.seminoncol.2014.08.004
305 Wozniak-Knopp G et al. (2010) Introducing antigen-binding sites in structural loops of
306 immunoglobulin constant domains: Fc fragments with engineered HER2/neu-binding sites
307 and antibody properties *Protein engineering, design & selection : PEDS* 23:289-297
308 doi:10.1093/protein/gzq005
309 Xiao X, Feng Y, Vu BK, Ishima R, Dimitrov DS (2009) A large library based on a novel
310 (CH2) scaffold: identification of HIV-1 inhibitors *Biochem Biophys Res Commun* 387:387-
311 392 doi:10.1016/j.bbrc.2009.07.044
312 Zielonka S, Empting M, Grzeschik J, Konning D, Barelle CJ, Kolmar H (2014a) Structural
313 insights and biomedical potential of IgNAR scaffolds from sharks mAbs:0
314 doi:10.4161/19420862.2015.989032
315 Zielonka S et al. (2014b) Shark Attack: High affinity binding proteins derived from shark
316 vNAR domains by stepwise in vitro affinity maturation *Journal of biotechnology*
317 doi:10.1016/j.jbiotec.2014.04.023

318

319

320

321

322

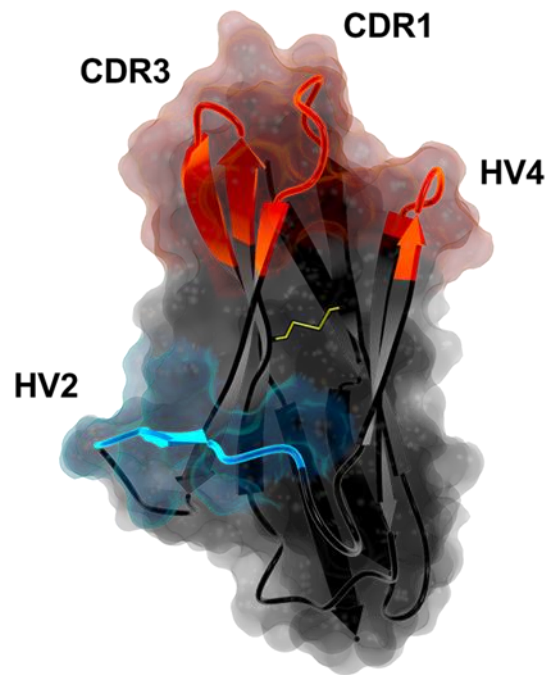
323

324

325

326

328

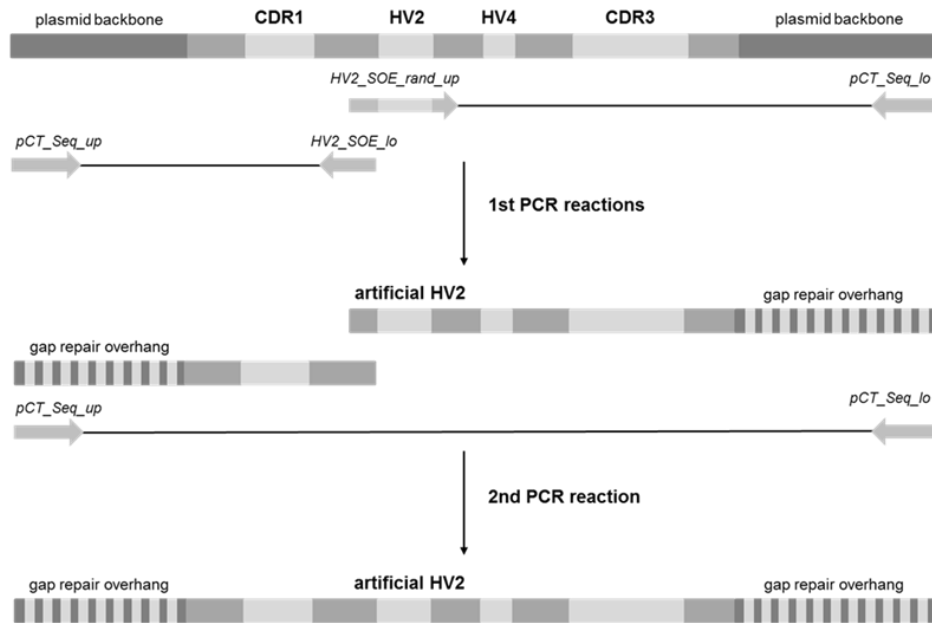
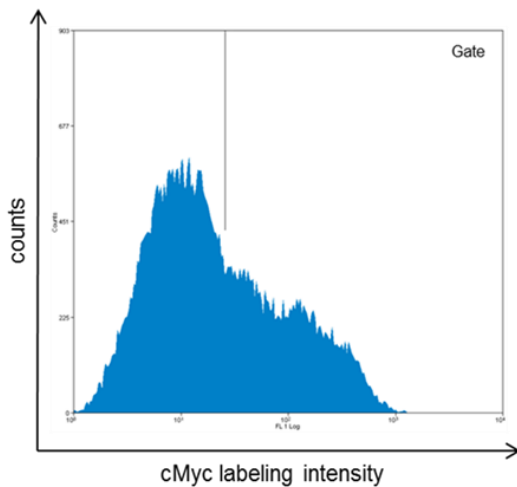
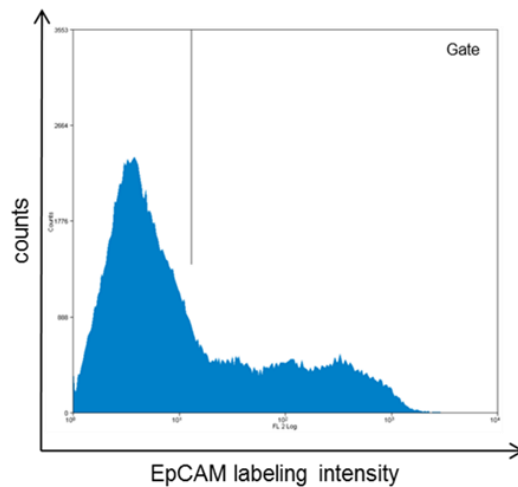


329

330

331 **Fig. 1** Depiction of the rationale for the generation of a new antigen-binding site into the vNAR scaffold. The
 332 conventional paratope composed of CDR3, CDR1 (and HV4) is shown in red. The potentially new antigen-
 333 binding site, consisting of HV2 is shown in blue. Yellow: Disulfide bond. Model based on pdb entry 4HGK
 334 (Kovalenko et al. 2013) generated using YASARA structure.(Krieger et al. 2009) Sequence shown for parental
 335 molecule 5005 used for library design. Sequence for CDR1 and CDR3 as well as HV4 of the conventional antigen-
 336 binding site shaded in red. Residues in sequence exposed loop corresponding to HV2 and considered for
 337 randomization shown in blue.

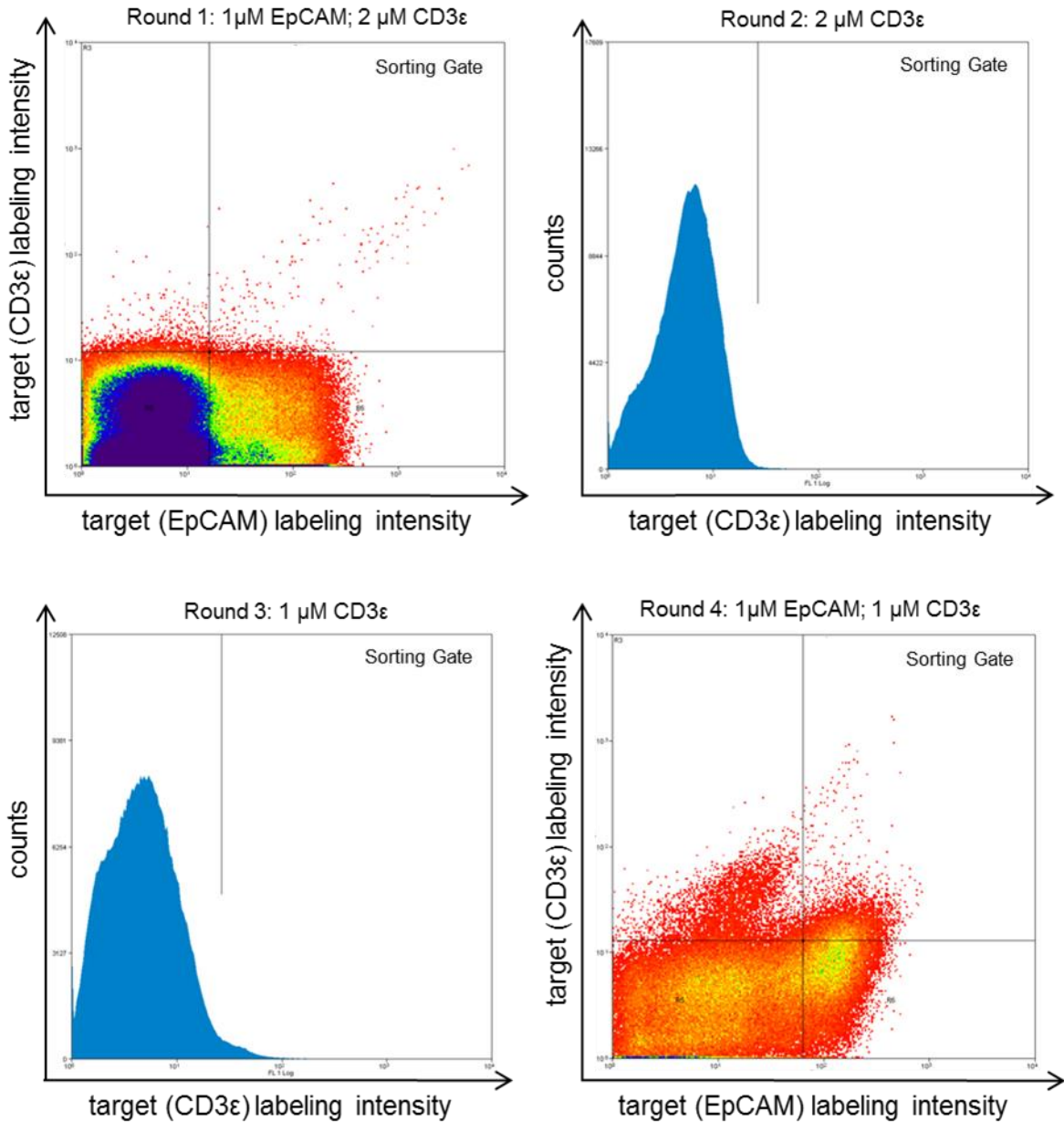
338

A**B****C**

339

340 **Fig. 2** (A) Schematic representation of PCR-based randomization of HV2. pCT plasmid encoding EpCAM-
 341 specific vNAR 5005 was used as template. In first PCRs HV2 was randomized and the corresponding up and low
 342 fragments of the vNAR domain were constructed. In a subsequent reaction the total vNAR molecule was
 343 constructed *via* splicing by overlap extension. (B and C) Analysis of HV2-randomized library based on EpCAM-
 344 specific vNAR 5005. Histogram of cMyc surface expression (B) and EpCAM-binding (C) of the constructed
 345 vNAR library assessed by indirect immunofluorescence labeling and flow cytometry, one day post induction. Cells
 346 in gate: 40.1 % for cMyc staining and 35.9 % for EpCAM-labeling (1 μ M EpCAM, detected with EpCAM-specific
 347 antibody clone HEA-125 conjugated to PE, Miltenyi Biotec).

348

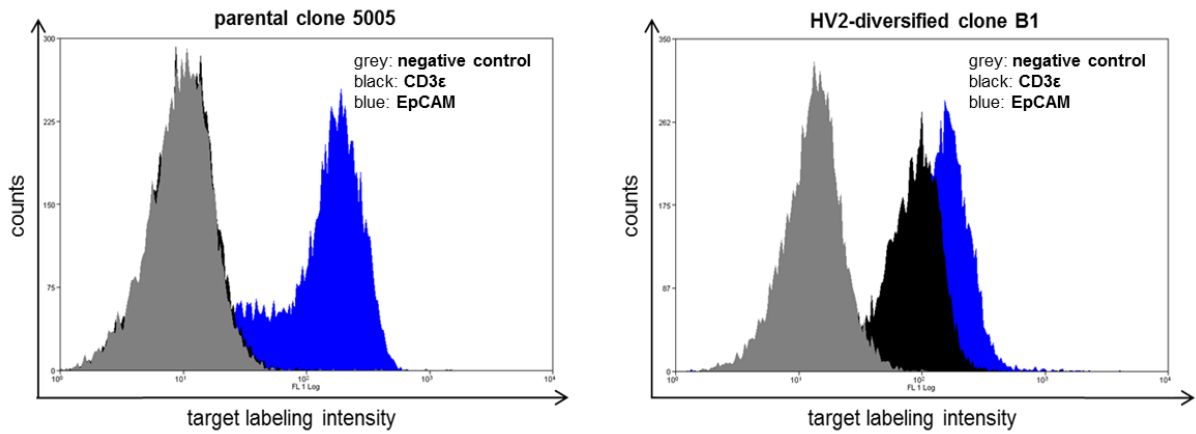


349

350 **Fig. 3** Screening of a HV2-randomized EpCAM-specific library based on vNAR 5005 against CD3 ϵ . Sorting gates
 351 and target concentrations are shown. In round one and four, cells were simultaneously labeled for EpCAM-binding
 352 using Penta-His Alexa Fluor 488 conjugate and CD3 ϵ -binding *via* biotinylated antigen and Steptavidin-APC. In
 353 round two and three, cells were only labeled for CD3 ϵ -binding using his-tagged antigen and Penta-His Alexa Fluor
 354 488 conjugate. After round 3 a resort was performed. Cells in the sorting gate were isolated, grown and induced
 355 for the next round of selection. Target-positive cells in sorting gate: (R1) 0.1 %; (R2) 0.17 %; (R3) 1.92 % and
 356 (R4) 5.8 %.

357

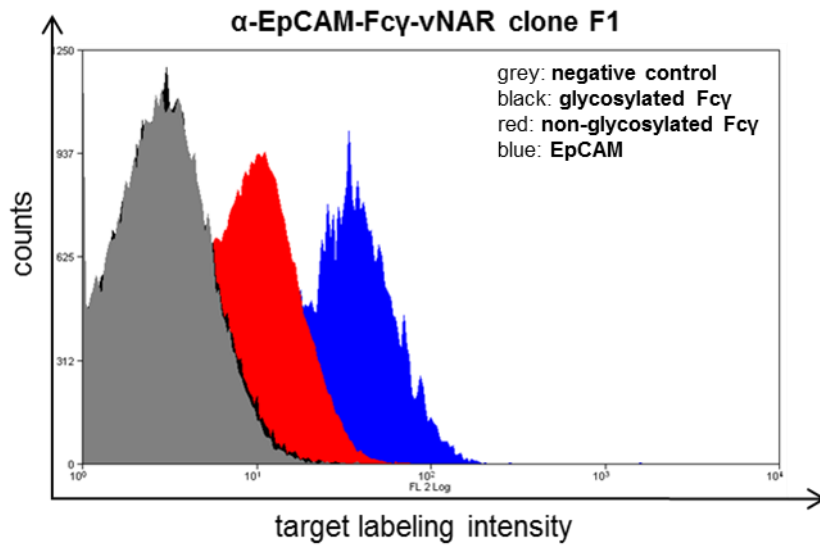
358



359

360 **Fig. 4** Single clone analysis of mono-specific, parental clone 5005 and HV2-diversified clone B1 for EpCAM and
 361 CD3ε-binding. Single clones were incubated with 1 μM of the respective antigen. Alexa Fluor 488 labeled anti-
 362 His-tag antibody was used for the detection of target binding. Blue: Cells stained with EpCAM. Black: Cells
 363 incubated with CD3ε. Grey: Negative control, cells only labeled with secondary detection antibody.

364



365

366 **Fig. 5** Single clone analysis of EpCAM- and non-glycosylated Fc γ -binding HV2-diversified clone F1. Single clone
 367 was incubated with 1 μ M of the respective antigen. Anti-human IgG conjugated to PE (Fc γ -specific) was used for
 368 the detection of target binding. Grey: Negative control, cells only labeled with secondary detection antibody.
 369 Black: Cells incubated with glycosylated Fc γ . Red: Cells labeled with non-glycosylated Fc γ . Blue: Cells labeled
 370 with EpCAM and detected *via* EpCAM-specific antibody clone HEA-125 conjugated to PE (Miltenyi Biotec).

371

372

373

374 **Tab. 1** Equilibrium dissociation constants (K_D) determined by yeast surface display for HV-diversified clones
 375 compared to parental clone 5005.

vNAR clone	Type of molecule	K_D [nM] EpCAM	K_D [nM] CD3ϵ/Fcγ
5005	Parental molecule	40 \pm 13	- (CD3 ϵ / Fc γ)
B1	After library screen CD3ϵ	46 \pm 8	422 \pm 60 (CD3 ϵ)
F1	After library screen human Fcγ	53 \pm 10	~ 2600 (Fc γ)

376
 377
 378
 379